ELSEVIER

Lithos 48 (1999) 217–235

LITHOS

Evidence from mantle xenoliths for relatively thin (< 100 km) continental lithosphere below the Phanerozoic crust of southernmost South America

Charles R. Stern [a,*], Rolf Kilian [b,1], Bettina Olker [c,2], Eric H. Hauri [d,3], T. Kurtis Kyser [e,4]

[a] Department of Geological Sciences, University of Colorado, Boulder, CO 80309-0399, USA
[b] Geologisches Institut, Universität Freiburg, D-79104 Freiburg, Germany
[c] Mineralogisches Institut, Universität Heidelberg, 69120 Heidelberg, Germany
[d] Department of Terrestrial Magnetism, Carnegie Institution of Washington, Washington, DC 20015, USA
[e] Department of Geological Sciences, Queen's University, Kingston, Ontario, Canada K7L 3N6

Received 6 April 1998; received in revised form 8 February 1999; accepted 9 February 1999

Abstract

Garnet peridotite xenoliths in the Quaternary Pali-Aike alkali olivine basalts of southernmost South America are samples of the deeper portion of continental lithosphere formed by accretion along the western margin of Gondwanaland during the Phanerozoic. Core compositions of minerals in garnet peridotites indicate temperatures of 970 to 1160°C between 1.9 and 2.4 GPa, constraining a geothermal gradient which suggests a lithospheric thickness of approximately 100 km below this region. Previously, this lithosphere may have been heated and thinned to ≤ 80 km during the Jurassic break-up of Gondwanaland, when widespread mafic and silicic volcanism occurred in association with extension in southern South America. Subsequent cooling, by up to > 175°C, and thickening, by about 20 km, of the lithosphere is reflected in low-temperature (< 970°C) spinel peridotites by chemical zonation of pyroxenes involving a rimward decrease in Ca, and in moderate- and high-temperature (> 970°C) peridotites by textural evidence for the transformation of spinel to garnet. A recent heating event, which probably occurred in conjunction with modal metasomatism related to the genesis of the Pali-Aike alkali olivine basalts, has again thinned the lithosphere to < 100 km. Evidence for this heating is preserved in moderate- and high-temperature (> 970°C) peridotites as chemical zonation of pyroxenes involving a rimward increase in Ca, and by kelyphitic rims around garnet. The majority of moderate- and high-temperature (> 970°C) xenoliths are petrochemically similar to the asthenospheric source of mid-oceanic ridge basalts: fertile (> 20% modal clinopyroxene and garnet), Fe-rich garnet lherzolite with major element composition similar to estimates of primitive mantle, but large-ion-lithophile and light-rare-earth element depletion relative to heavy-rare-earth elements, and with Sr, Nd, Pb, Os, and O isotopic compositions similar to MORB. In contrast, infertile, Mg-rich spinel harzburgite is predominant among low-temperature (< 970°C) xenoliths. This implies a significant chemical gradient and increasing density with depth in the mantle section

* Corresponding author. Fax: +1-303-492-2606; E-mail: sternc@stripe.colorado.edu
1 Fax: +49-0761-2036496; E-mail: kilianr@sun2.ruf.uni-freiburg.de.
2 Fax: +49-6221-544805; E-mail: bolker@classic.min.uni-heidelberg.de.
3 Fax: +1-202-364-8726; E-mail: hauri@dtm.ciw.edu.
4 Fax: +1-613-533-6592; E-mail: kyser@geol.queensu.ca.

PII: S0024-4937(99)00030-4

represented by the xenoliths, and the absence of a deep, low density, olivine-rich root below the southernmost South American crust such as has been inferred below Archean cratons. With respect to both temperature/rheology and chemistry/density, the subcontinental mantle lithosphere below southernmost South America is similar to that below oceanic crust. It is interpreted to have formed by tectonic capture, during the Paleozoic, of a segment of what had previously been oceanic lithosphere generated at a late Proterozoic mid-oceanic spreading ridge.

Keywords: Mantle; Lithosphere; Peridotite; Xenolith; South America

1. Introduction

Garnet peridotite xenoliths from the Quaternary Pali-Aike alkali olivine basalt field, southernmost South America (Fig. 1), provide a unique window into the deeper portions of subcontinental lithosphere in a region where crustal rocks are Phanerozoic in age (de Wit, 1977; Ramos, 1988). Based on mineral thermometry and barometry, Skewes and Stern (1979), Stern et al. (1986, 1989), and Douglas et al. (1987) concluded that the subcontinental mantle lithosphere below this region has a high geothermal gradient of > 10°C/km between 50 and 100 km depth, with temperature of > 1300°C at depths of

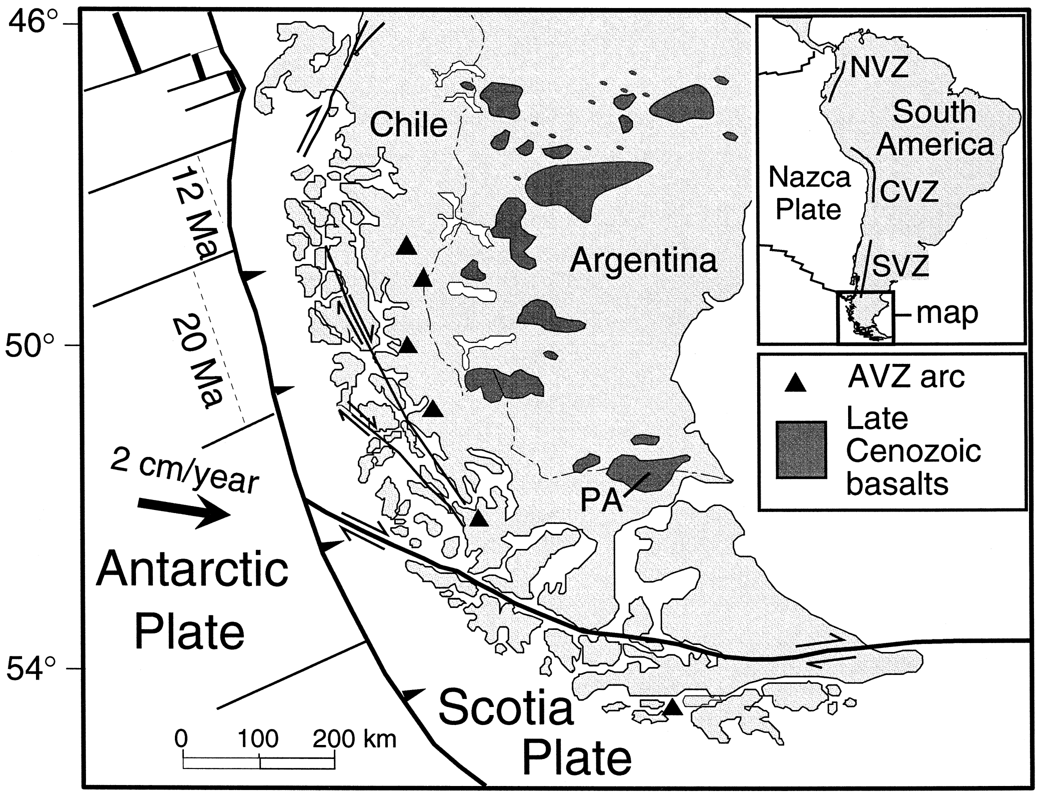

Fig. 1. Map of southern South America showing the location of the Quaternary Pali-Aike (PA) alkali olivine basalt field, from which the xenoliths discussed in this paper were obtained, and other late Cenozoic basalts of the Patagonian plateau lavas (Stern et al., 1986, 1989, 1990). Also shown are tectonic features such as plates, plate boundaries (Cande and Leslie, 1986), and the adakitic stratovolcanoes of the Andean Austral Volcanic Zone (AVZ; Stern and Kilian, 1996).

< 100 km (Fig. 2), suggesting the lack of a deep subcontinental lithospheric root below this region of southernmost South America.

Xenoliths in the Pali-Aike basalts are dominantly harzburgites and lherzolites, along with minor websterites and pyroxenites. Stern et al. (1986, 1989) demonstrated that with increasing depth in the subcontinental lithosphere below southernmost South America, the proportion of denser, more fertile lherzolite increases relative to less dense, less fertile harzburgite. They concluded that the deepest portion of this subcontinental lithosphere consists of fertile garnet lherzolite with major element composition similar to ''pyrolite'' and trace-element and isotopic characteristics similar to the global asthenospheric mantle source of mid-ocean ridge basalts.

Thus with respect to both temperature/rheology and chemistry/density, the subcontinental mantle

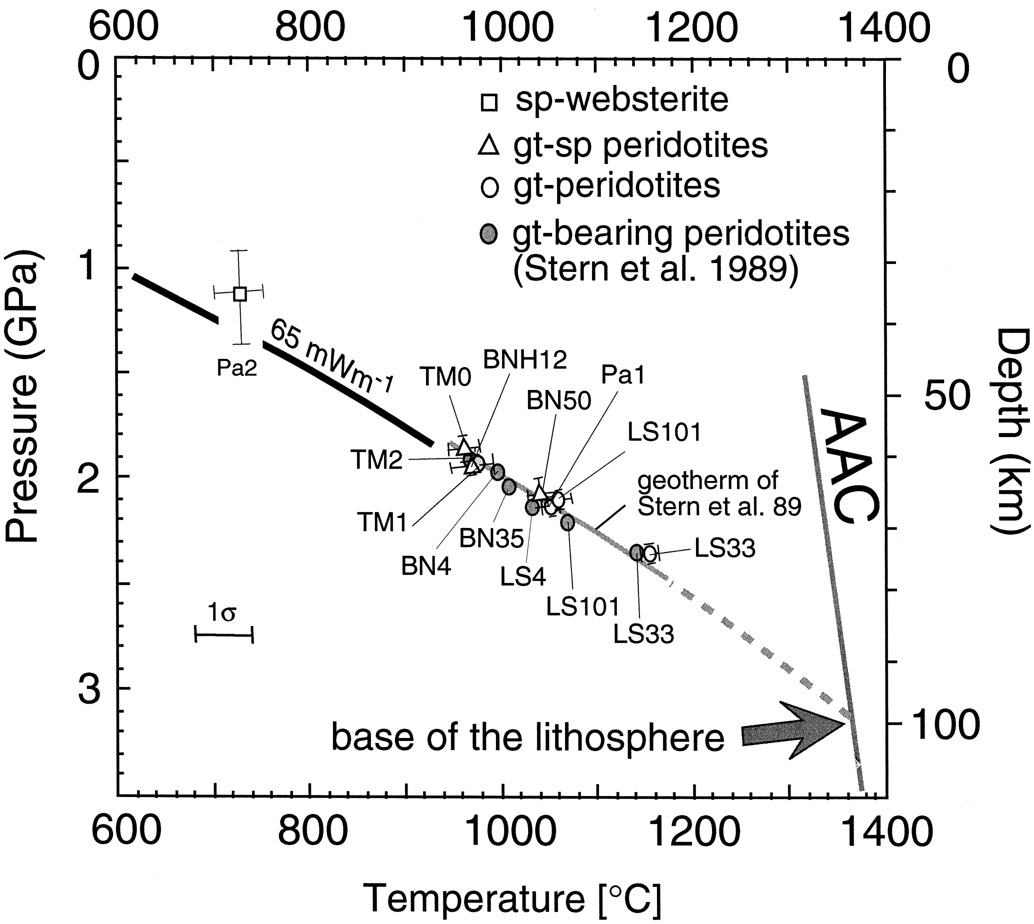

Fig. 2. Estimates of the temperature and pressure of equilibration of Pali-Aike garnet peridotites (open symbols) based on the Ca-in-orthopyroxene thermometer and Al-in-orthopyroxene barometer of Brey and Köhler (1990) as applied to mineral core compositions (Olker, 1997). For the spinel websterite Pa2, pressure was estimated based on the Ca-in-olivine barometer and temperature estimated with the two-pyroxene thermometer of Brey and Köhler (1990). These T and P estimates plot close to the 65-mW m^{-1} geotherm of Chapman (1986), and the geotherm they define (dashed line) intersects the adiabatic upwelling curve (AAC) of McKenzie and Bickle (1988) at about 100 km, implying a thin lithosphere below Pali-Aike. This geotherm is similar to a previous one (solid symbols; Stern et al., 1989) based on independent microprobe mineral composition data and calculated with a different two-pyroxene thermometer (Wells, 1977) and the garnet–orthopyroxene barometer (Nickel and Green, 1985). As discussed in the text, the base of the lithosphere below Pali-Aike has recently been heated to higher temperatures than those implied by core compositions of xenolith minerals, and thinned to < 100 km (see Fig. 9).

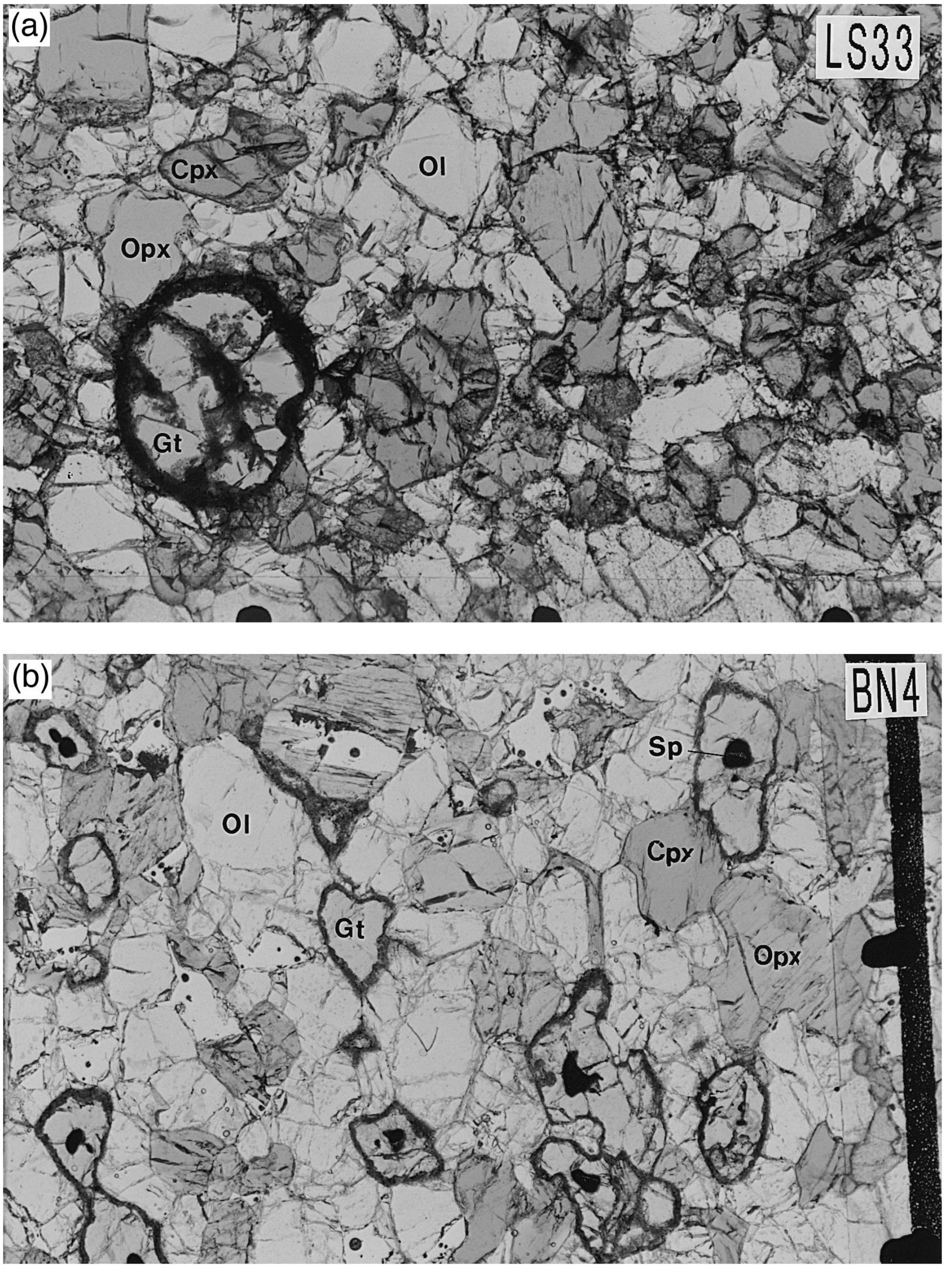

Fig. 3. Photomicrographs of three garnet peridotites from Pali-Aike. Garnet lherzolite LS33, which is the highest temperature (1160 to 1220°C; Figs. 2 and 4) xenolith documented, has a weakly porphyroclastic, but unfoliated texture. Moderate-temperature (990°C; Fig. 2) spinel + garnet lherzolite BN4 also has equigranular texture. The spinel + garnet harzburgite TM15 is cut by a high-Ti phlogopite vein. The photomicrographs of LS33 and BN4 are both 3 cm across, while that of TM15 is 4 cm across. Minerals are Ol = Mg–olivines (clear), Opx = Mg–orthopyroxenes (grey, olive green in thin section), Cpx = Cr–diopside clinopyroxene (grey, emerald green in thin section), Gt = pyrope garnets (grey, reddish in thin section), Phl = phlogopite (dark brown to reddish brown in thin section due to their high-Ti content), and Sp = spinels (opaque).

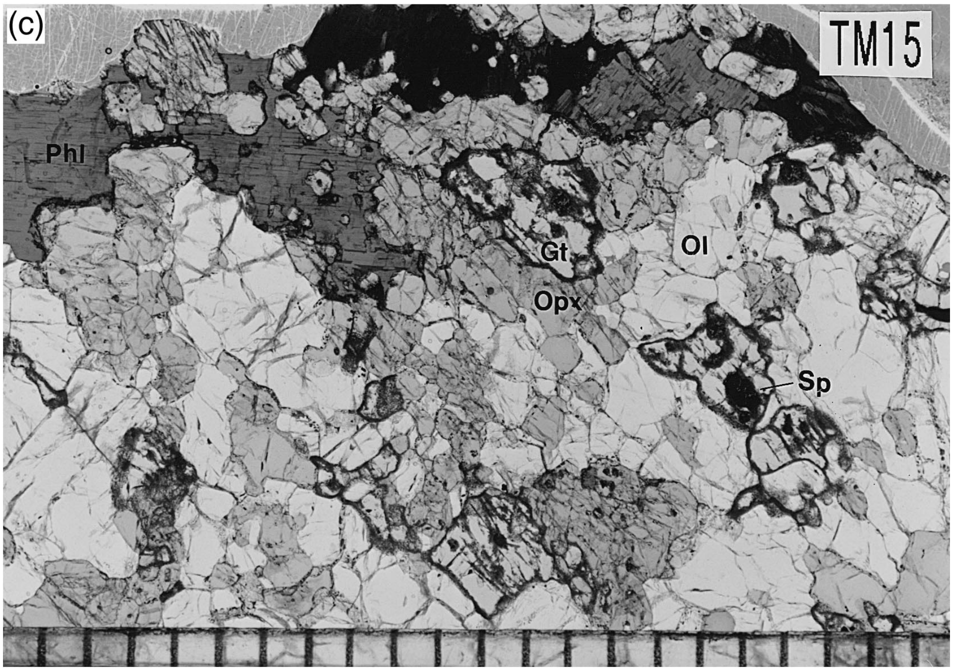

Fig. 3 (continued).

lithosphere below southernmost South America is apparently similar to that below oceanic crust and distinctly different from that below Archean cratons. This paper presents the results of new electron and ion microprobe determinations of mineral chemistry and new Sr, Nd, Pb, Os and O isotopic data that substantiate the conclusion that not all continental crust is underlain by a thick ($\gg 100$ km) lithospheric mantle root.

2. Xenolith petrochemistry

2.1. Xenolith mineralogy and lithology

Xenoliths in the Pali-Aike basalts include sedimentary and granitic rocks, mafic and silicic meta-igneous granulites (Selverstone and Stern, 1983), pyroxenites, olivine websterites, and mantle-derived Type I Cr–diopside peridotites (Skewes and Stern, 1979; Stern et al., 1986, 1989). Eclogites are scarce. Secondary effects such as melt infiltration or grain boundary melting related to heating, decompression and reaction with the basaltic host during transport to the surface are either minimal or absent in most peridotite xenoliths, as is weathering or serpentinization. The peridotites generally have coarse equigranular textures (Fig. 3), and are not strongly foliated (Douglas et al., 1987).

Peridotites include spinel, spinel + garnet, and garnet harzburgites and lherzolites consisting dominantly of Mg–olivine (Fo85–92), orthopyroxene (En82–90), Cr–diopside clinopyroxene, Cr–pyrope garnet and spinel, as well as minor pargasitic amphibole and Ti–phlogopite mica which occur both in veins (sample TM15 in Fig. 3) and as isolated mineral grains. Representative electron microprobe analysis of mineral major-element chemistry in Pali-Aike peridotite xenoliths have been presented in the works of Skewes and Stern (1979), Douglas et al. (1987) and Stern et al. (1989). Spinels include both high-Al/low-Cr types, which occur exclusively in low-temperature ($< 970°C$) garnet-free peridotites, and also low-Al/high-Cr types, which occur in moderate- and high-temperature ($> 970°C$) peridotites (Stern et al., 1986). Spinel in garnet + spinel xenoliths is always the low-Al/high-Cr type and is typically fully enclosed as inclusions in garnet (samples BN4 and TM15 in Fig. 3). These spinels are interpreted as relics of the reaction spinel + pyroxene ⇒ garnet + olivine. Also, garnet in peridotites without spinel often have inclusions of olivine, suggesting that they formed by the same reaction from originally spinel-bearing peridotites. This reaction may result from either cooling, pressure increase, or both, indicating a multi-stage thermal history for the lithosphere below Pali-Aike, as discussed in more detail below. Exsolution of clinopyroxene from orthopyroxene, and vice versa, in some low-temperature (< 970°C) spinel peridotites and olivine websterites, is also considered to be mineralogic evidence for cooling. In contrast, garnets in relatively high-temperature (> 970°C) garnet peridotites have kelyphitic rims containing pyroxenes and spinel, suggesting an increase in temperature.

New electron microprobe analysis, which involved systematic rim-to-core-to-rim profiles of olivines, pyroxenes, spinels and garnets, indicate that core compositions of minerals are consistent with previously published analyses, but that different xenoliths have distinctive core-to-rim chemical zonations. These zonations involve the elements Al and Ca (Fig. 4), but not Fe or Mg, possibly due to the more rapid diffusion rates of these latter elements (Sautter and Harte, 1988; Witt-Eickschen and Seck, 1991; Werling and Altherr, 1997). Furthermore, Al and Ca zonations are much more pronounced in orthopyroxene than in clinopyroxene, reflecting differences in the diffusion rates of these cations between both pyroxene types (Werling and Altherr, 1997). Some spinel peridotites and olivine websterites, those that equilibrated at relatively low temperatures (< 970°C), have orthopyroxenes characterized by broad homogeneous cores and decreasing Al and Ca contents across the rims (LS-2; Fig. 4). In contrast, orthopyroxenes from high-temperature (> 970°C) spinel and garnet peridotites have increasing Al and Ca contents from their cores to their rims, but this zoning pattern is parabolic, and these grains do

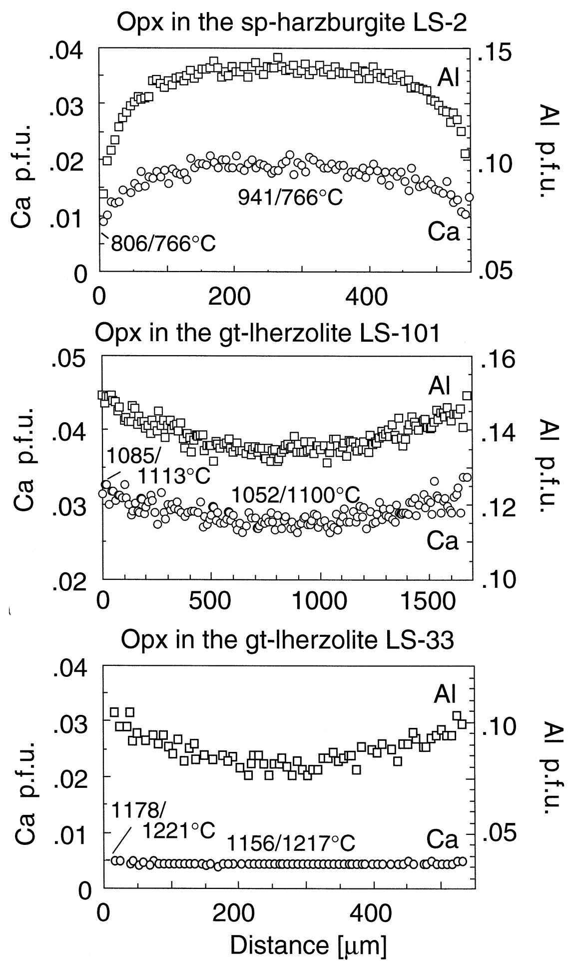

Fig. 4. Rim-to-rim zonations in Ca (circles) and Al (squares) concentrations (pfu = per formula unit) across orthopyroxene grains in spinel and garnet peridotites as determined by electron microprobe profiles. Core and rim temperatures were calculated by applying both the Ca-in-orthopyroxene and two-pyroxene thermometers of Brey and Köhler (1990); the former listed to the left of the slash, the latter to the right. Based on analysis of multiple pairs of grains, errors in the calculated temperatures are estimated as ±20°C for the cores (which may or may not be true cores) and ±12°C for the rims. As discussed in the text, the two-pyroxene thermometer is considered to more closely approach final equilibration temperature since Mg exchange between orthopyroxene and clinopyroxene is more rapid than Ca diffusion in orthopyroxene. For the low-*T* spinel peridotite LS2, the rim indicates a lower temperature than the core as estimated by the Ca-in-orthopyroxene thermometer, and the two-pyroxene thermometer gives a significantly lower temperature, because Ca diffusion slowed during progressive cooling. For the high-*T* garnet-bearing xenoliths, the rim indicates higher temperature than the core and the two-pyroxene thermometer gives higher temperatures because Ca diffusion has not kept pace with Mg exchange between the two pyroxenes during heating.

Table 1

Compositions of Pali-Aike peridotites, published estimates of Primitive Mantle, and averages of other spinel and garnet peridotites (Hofm = Hofmann (1988); Allègre = Allègre et al. (1995); P&M = Palme and Nickel (1985); Ringw = Ringwood (1979); McDon = McDonough (1990); SpP-1 and SpP-2 = Average continental spinel peridotites (Maaløe and Aoki, 1975; McDonough, 1990); GtP-1 = Average continental garnet peridotites (M&A = Maaløe and Aoki, 1975); Lherz = Average Pali-Aike (PA) garnet-bearing lherzolite; Stern = determined by wet chemical analysis (Stern et al., 1989); Olker (1997) and Kilian = independent XRF determinations using standards JP-6 and SARM47, Heidelberg University)

	Estimates of the Primitive Mantle					Peridotite averages			Spinel harzburgites					Spinel–garnet harzburgites			
	Hofm	Allègre	P&M	Ringw	McDon	SpP-1	SpP-2	GtP-1	PA 3	LS-0	PA-5	PA-6	LS-1	BN 50		TM15	TM16
	1988	1995	1986	1979	1990	M&A	McDon	M&A	Olker	Kilian	Kilian	Kilian	Kilian	Olker	Kilian	Olker	Olker
SiO_2	45.96	46.12	46.20	45.10	44.8	44.15	44.0	44.99	43.95	44.79	43.96	44.49	43.31	42.23	42.25	44.92	47.34
TiO_2	0.18	0.18	0.23	0.20	0.21	0.07	0.09	0.06	0.05	0.04	0.04	0.02	0.04	0.16	0.17	0.13	0.23
Al_2O_3	4.06	4.09	4.75	3.30	4.45	1.96	2.27	1.40	1.03	1.00	0.95	0.87	0.52	3.83	3.99	2.97	3.27
FeO_{tot}	7.54	7.49	7.70	8.00	8.40	8.28	8.43	7.89	7.58	7.23	7.14	7.21	6.80	9.56	9.33	9.24	8.73
MnO	0.20	0.15	0.13	0.15	0.14	0.12	0.14	0.11	0.12	0.12	0.11	0.11	0.10	0.13	0.13	0.13	0.13
MgO	37.78	37.77	35.50	38.10	37.2	42.25	41.40	42.60	44.86	45.13	45.30	45.96	47.64	41.00	40.74	40.01	39.06
CaO	3.21	3.23	4.36	3.10	3.60	2.08	2.15	0.82	0.79	0.68	0.88	0.63	0.40	0.87	0.98	0.69	0.81
Na_2O	0.33	0.36	0.40	0.40	0.34	0.11	0.24	0.05	0.02	0.07	0.06	0.01	0.00	0.00	0.01	0.04	0.05
K_2O	–	0.03	–	–	0.03	0.05	0.05	0.11	0.02	0.00	0.00	0.01	0.00	0.00	0.00	0.00	0.09
Cr_2O_3	–	0.38	0.43	0.40	0.43	0.44	0.39	0.32	0.46	0.46	0.42	0.31	0.34	0.79	0.81	0.33	0.37
NiO	0.26	0.25	0.23	–	0.24	0.27	0.27	0.26	0.32	0.27	0.29	0.28	0.33	0.32	0.32	0.27	0.24
Sum	99.92	100.5	99.93	98.75	99.84	99.78	99.43	99.79	99.15	99.78	99.13	99.91	99.48	98.88	98.74	98.73	100.32
Mg#	89.9	89.9	89.2	89.5	88.8	90.1	89.8	90.6	91.3	91.8	91.9	91.9	92.6	88.4	88.6	88.5	88.9

	Garnet lherzolites						Garnet–spinel lherzolites										Lherz
	LS101			LS33			BN4	BN35	BNH12	LS4	Pa1	TM0	TM1		TM2		PA
	Olker	Stern	Kilian	Olker	Stern	Kilian	Stern	Stern	Olker	Stern	Olker	Olker	Stern	Olker	Stern	Olker	aver.
SiO_2	44.04	45.60	44.20	44.81	44.80	45.65	45.30	45.40	43.86	44.90	44.01	44.63	45.00	44.20	45.30	44.00	44.74
TiO_2	0.08	0.12	0.09	0.11	0.16	0.13	0.20	0.25	0.14	0.20	0.16	0.15	0.20	0.15	0.17	0.12	0.15
Al_2O_3	2.77	3.90	1.50	3.37	3.90	3.48	4.60	4.30	2.10	3.80	3.59	2.86	4.10	3.66	4.00	2.75	3.39
FeO_{tot}	7.96	8.20	8.02	7.60	8.10	7.59	8.70	8.30	8.83	7.90	7.85	8.01	8.20	7.89	8.60	8.22	8.11
MnO	0.13	0.16	0.11	0.13	0.14	0.13	0.18	0.14	0.12	0.12	0.11	0.12	0.15	0.13	0.14	0.12	0.13
MgO	41.27	37.90	42.12	39.39	37.30	39.23	36.90	37.10	40.81	38.20	39.45	39.21	37.60	38.33	37.20	39.98	38.91
CaO	1.81	3.00	2.57	2.28	3.00	2.65	3.40	3.30	2.30	2.90	3.06	3.12	3.20	3.05	3.00	2.61	2.84
Na_2O	0.11	0.25	0.21	0.15	0.26	0.19	0.29	0.30	0.16	0.22	0.27	0.28	0.31	0.25	0.27	0.20	0.23
K_2O	0.00	0.00	0.00	0.00	0.00	0.00	0.00	0.00	0.02	0.00	0.00	0.00	0.00	0.01	0.00	0.00	0.00
Cr_2O_3	0.38	0.42	0.28	0.46	0.42	0.43	0.41	0.30	0.45	0.49	0.41	0.34	0.33	0.38	0.39	0.31	0.39
NiO	0.32	0.32	0.27	0.26	0.25	0.24	0.26	0.24	0.29	0.28	0.26	0.27	0.28	0.25	0.32	0.26	0.27
Sum	98.87	99.97	99.37	98.56	98.33	99.71	100.24	99.57	99.07	99.01	99.17	98.99	99.37	98.30	99.39	98.57	99.17
Mg#	90.2	89.2	90.4	90.2	89.1	90.2	88.3	88.9	89.2	89.6	90.0	89.7	89.1	89.7	88.5	89.7	89.5

not contain a broad homogeneous core (LS101; Fig. 4). In the highest temperature xenoliths (LS33; Fig. 4), only the Al content of orthopyroxene grains is zoned. These different core-to-rim chemical zonation

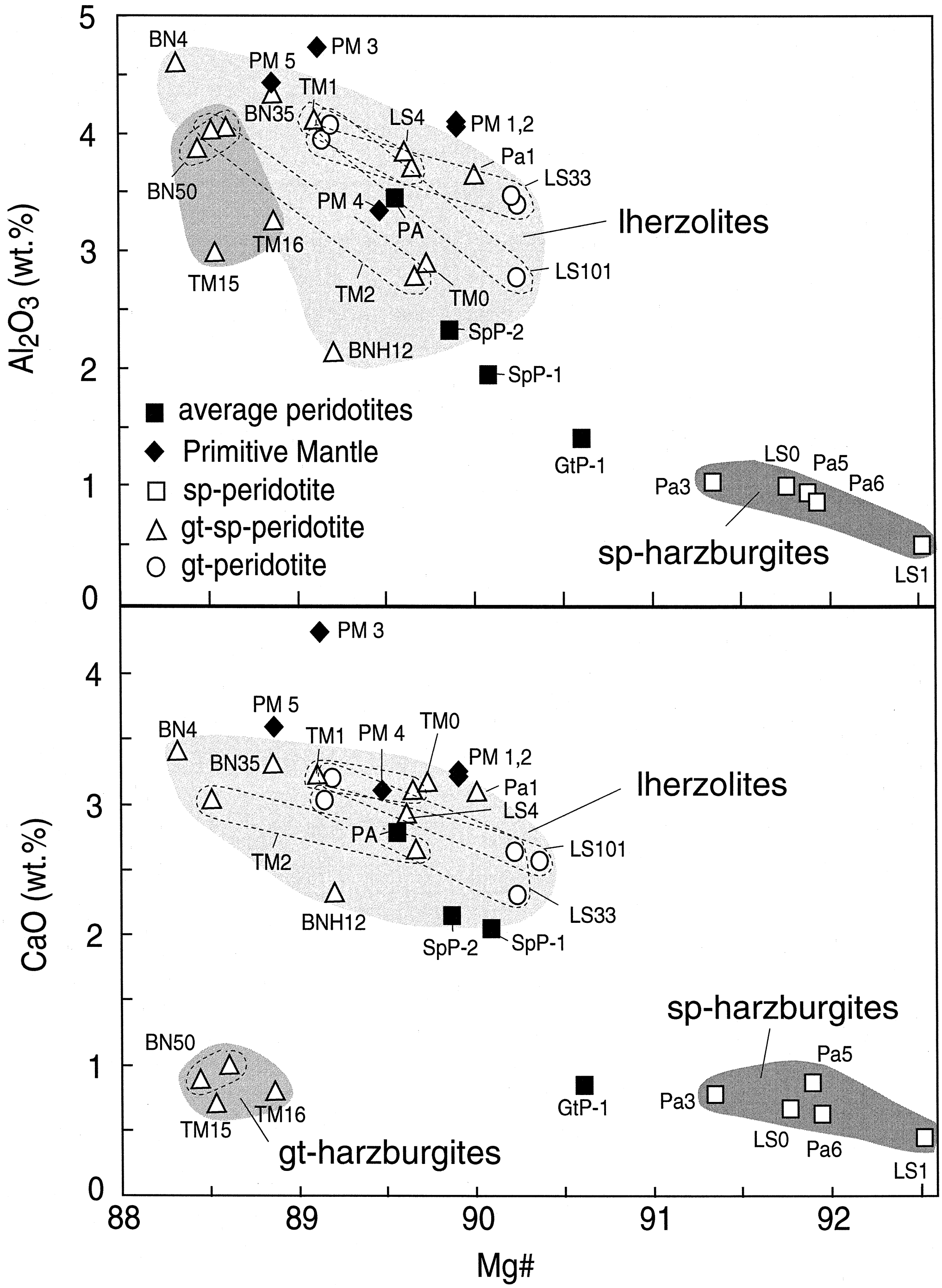

patterns are significant for the interpretation of the complexities of the thermal history of the mantle lithosphere below the Pali-Aike volcanic field.

Table 1 presents previously published (Stern et al., 1989) and new major element chemical analysis of 18 vein-free peridotite xenoliths from Pali-Aike including both garnet-bearing and garnet-free lherzolites and harzburgites, as well as the average composition of Pali-Aike garnet-bearing lherzolites, other published averages of continental spinel and garnet peridotites, and estimates of the major element composition of primitive mantle. Pali-Aike garnet-bearing lherzolites have major-element compositions similar to estimates of primitive mantle, and significantly higher CaO and Al_2O_3, and lower Mg# compared to previously published compilations of the average composition of either spinel or garnet lherzolites from continental lithosphere (Fig. 5). Compared to Pali-Aike garnet lherzolites, spinel harzburgites have lower CaO and Al_2O_3, and higher Mg# (Fig. 5), consistent with significant amounts of melt extraction (McDonough, 1990). Garnet-bearing harzburgites, in contrast, have lower CaO, but not lower Al_2O_3 or higher Mg#.

Modal metasomatism has produced veins containing high-Ti phlogopite ± pargasitic amphibole ± ilmenite in some peridotite xenoliths (sample TM15 in Fig. 3), as well as disseminated phlogopite and amphibole (Stern et al., 1986, 1989). Such veins are more abundant in moderate- and high-temperature (> 970°C) xenoliths than in low-temperature ones. The volume of vein material may be up to 3% in some xenoliths. This metasomatism has added Ti, K, and Na, as well as H_2O and some trace-elements to the mantle, which is not reflected in the major element analysis of the vein-free peridotites presented in Table 1.

Table 2
Trace-element contents, in ppm, of garnet and clinopyroxene in fertile high-temperature garnet lherzolites LS101 and LS33, and infertile moderate-temperature spinel harzburgite Pa5. Determined by LAM–ICP–MS at Memorial University, Newfoundland. Class standards NBS612 and BCR2 were used for calibration. Techniques described by Jackson et al. (1992) and Taylor et al. (1996)

Sample	LS101	LS33	LS101	LS33	PA5	PA5
Mineral	gt-core	gt-core	cpx-core	cpx-core	cpx-core	cpx-rim
Th	0.14	0.01	0.05	0.06	0.03	0.32
U	0.05	0.02	0.01	0.01	< 0.01	0.08
Nb	1.35	1.21	0.85	0.61	0.48	3.77
Ta	0.04	0.04	0.18	0.09	0.08	0.40
La	0.03	0.05	1.69	1.57	0.97	4.36
Ce	0.65	0.59	6.98	5.55	4.27	11.36
Pr	0.21	0.20	1.06	0.99	0.89	1.97
Nd	2.16	2.11	4.28	5.31	4.39	8.82
Sm	2.63	2.85	1.42	1.40	1.69	2.66
Eu	1.15	1.57	0.50	0.49	0.59	0.89
Gd	6.29	6.73	1.37	1.84	1.84	2.52
Tb	2.06	1.80	0.20	0.28	0.29	0.39
Dy	19.68	14.18	0.82	1.42	1.38	1.74
Ho	6.17	3.97	0.14	0.28	0.22	0.31
Er	20.71	11.80	0.20	0.66	0.47	0.63
Tm	3.88	2.22	0.03	0.10	0.06	0.08
Yb	24.54	12.73	0.35	0.47	0.24	0.47
Lu	3.99	2.06	0.02	0.05	0.04	0.05

2.2. Trace-element and isotope chemistry

Stern et al. (1989) determined that fertile garnet-bearing lherzolites from Pali-Aike have whole-rock Sm/Nd, $^{87}Sr/^{86}Sr$ and $^{143}Nd/^{144}Nd$ ratios similar to mid-ocean ridge basalts. New laser ablation microprobe–inductively coupled plasma–mass spectrometry (LAM–ICP–MS) analysis of trace-elements in clinopyroxene and garnet (Table 2; Fig. 6), and of the Sr and Nd isotopic composition of leached

Fig. 5. Whole-rock CaO and $Al_2 0_3$ contents of Pali-Aike xenoliths (open symbols) plotted against Mg# and compared with both different estimates for the Primitive Mantle (solid diamonds, data from Table 1; PM1, Hofmann, 1988; PM2, Allègre et al., 1995; PM3, Palme and Nickel, 1985; PM4, Ringwood, 1979; PM5, McDonough, 1990), and published compilations of the average compositions of continental spinel and garnet peridotite xenoliths (solid squares, data from Table 1; SpP-1 and GtP-1, Maaløe and Aoki, 1975; SpP-2, McDonough, 1990). Samples with multiple analysis (LS33, LS101, TM1, TM2 and BN50) are connected by dashed lines and the average of Pali-Aike garnet lherzolites is indicated by the solid square PA. The figure illustrates the major element similarity between fertile garnet-bearing lherzolites from Pali-Aike and estimates of Primitive Mantle, and significant differences between these lherzolites and both garnet and spinel harzburgites.

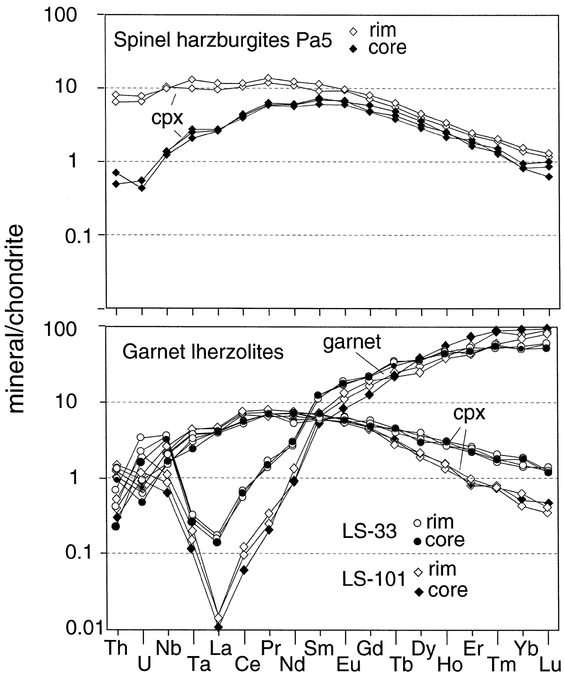

Fig. 6. Trace-element compositions, normalized to chondritic abundances (Taylor and McLennan, 1985), of both cores (solid symbols) and rims (open symbols) of garnet and clinopyroxene in spinel and garnet peridotites (Table 2). Minerals in fertile, high temperature, garnet lherzolites are unzoned, while those in the infertile, lower temperature spinel harzburgites show rim enrichment of the more incompatible elements.

clinopyroxene and garnet separates from garnet-bearing lherzolites (Table 3; Fig. 7), confirm this conclusion. For garnet and clinopyroxene in garnet lherzolite LS33, Nd and Sm concentrations measured independently by LAM–ICP–MS and isotope dilution MS differ by $< 10\%$.

New Pb (Table 4; Fig. 8), Os (Table 5), and O (Table 6; Fig. 7) isotopic analysis also indicate that Pali-Aike garnet lherzolites are isotopically similar to MORB. Whole-rock O isotopic compositions were calculated from measured mineral values and estimated modal proportions. Inter-mineral differences in $\delta^{18}O$ have been discussed by Kyser (1990). Rhenium depletion ages for garnet lherzolites, calculated assuming $Re/Os = 0$, range from 0 to 860 Ma (Table 5), suggesting a late Proterozoic to Phanerozoic age for the mantle lithosphere below southernmost South America, consistent with the Phanerozoic age of the crustal rocks is this region (Ramos, 1988).

Infertile spinel harzburgites have similar O isotopic compositions as garnet-bearing lherzolites (Table 6; Fig. 7), but they have significantly lower whole-rock Sr, Nd and Sm concentrations, Sm/Nd and $^{143}Nd/^{144}Nd$ ratios, and higher $^{87}Sr/^{86}Sr$ ratios (Table 3; Fig. 7). The Nd and Sr isotopic ratios of these xenoliths are similar to Quaternary alkali olivine basalts from Patagonia (Fig. 7) and within the mantle array defined by oceanic basalts (Stern et al., 1989). The Os isotopic composition of one infertile spinel harzburgite indicates an older model age for this sample compared to the fertile garnet lherzolites.

High-Ti phlogopite and pargasitic amphibole from metasomatic veins within Pali-Aike xenoliths have

Table 3
Rb, Sr, Nd and Sm concentrations, in ppm, and Sr and Nd isotopic compositions of Pali-Aike peridotites (WR = whole-rock; Gt = garnet; Sp = spinel; Cpx = clinopyroxene; Phlg = phlogopite mica; Amp = amphibole)

Sample	Rb	Sr	$^{87}Sr/^{86}Sr$	Nd	Sm	$^{143}Nd/^{144}Nd$
Garnet peridotites (unveined)						
LS-33 WR	0.23	14.4	0.70298	0.942	0.295	0.51296
LS-33 Cpx	0.07	87.3	0.70298	5.34	1.37	0.51298
LS-33 Gt	0.02	0.31	–	2.04	2.49	0.51295
Spinel + garnet peridotites (unveined)						
TM-0 Cpx	–	82.2	0.70264	4.94	–	0.51313
TM-1 WR1	0.16	13.6	0.70292	0.840	0.324	0.51303
TM-1 WR2	0.26	12.0	0.70289	0.718	0.278	0.51303
TM-2 WR	0.16	12.7	0.70270	0.802	0.252	0.51297
Spinel peridotites (unveined)						
LS-2 WR	0.28	6.95	0.70362	0.391	0.097	0.51278
LS-20 WR	0.08	4.85	0.70365	0.436	0.099	0.51281
LS-6 WR	–	2.80	0.70373	0.200	0.042	0.51284
X-3 WR	–	6.32	0.70431	0.371	–	0.51281
BN-71 WR	–	2.54	0.70349	0.202	0.051	0.51291
BN-71 Cpx	0.02	61.8	0.70345	3.83	1.28	0.51288
Modally metasomatized (veined) peridotites						
BN-35 WR[a]	0.24	13.5	0.70338	1.136	0.374	0.51284
BN-72 WR[a]	–	6.81	0.70350	0.493	0.112	0.51285
BN-44 WR[a]	–	–	0.70343	–	–	0.51287
TM-16 Cpx[a]	–	94.9	0.70324	–	–	0.51301
TM-16 Phlg	–		0.70336	–	–	0.51292
TM-15 Cpx[a]	0.22	68.0	0.70325	4.58	1.56	0.51308
TM-15 Amp	20.2	251.3	0.70329	5.28	2.03	0.51293
TM-15 Phlg	201	52.4	0.70344	–	–	0.51291
BN-63 Phlg	248	33.2	0.70344	0.309	0.071	0.51284
BN-40 Phlg	230	32.7	0.70343	–	–	0.51287

[a] WR and Cpx measured for material outside the vein.

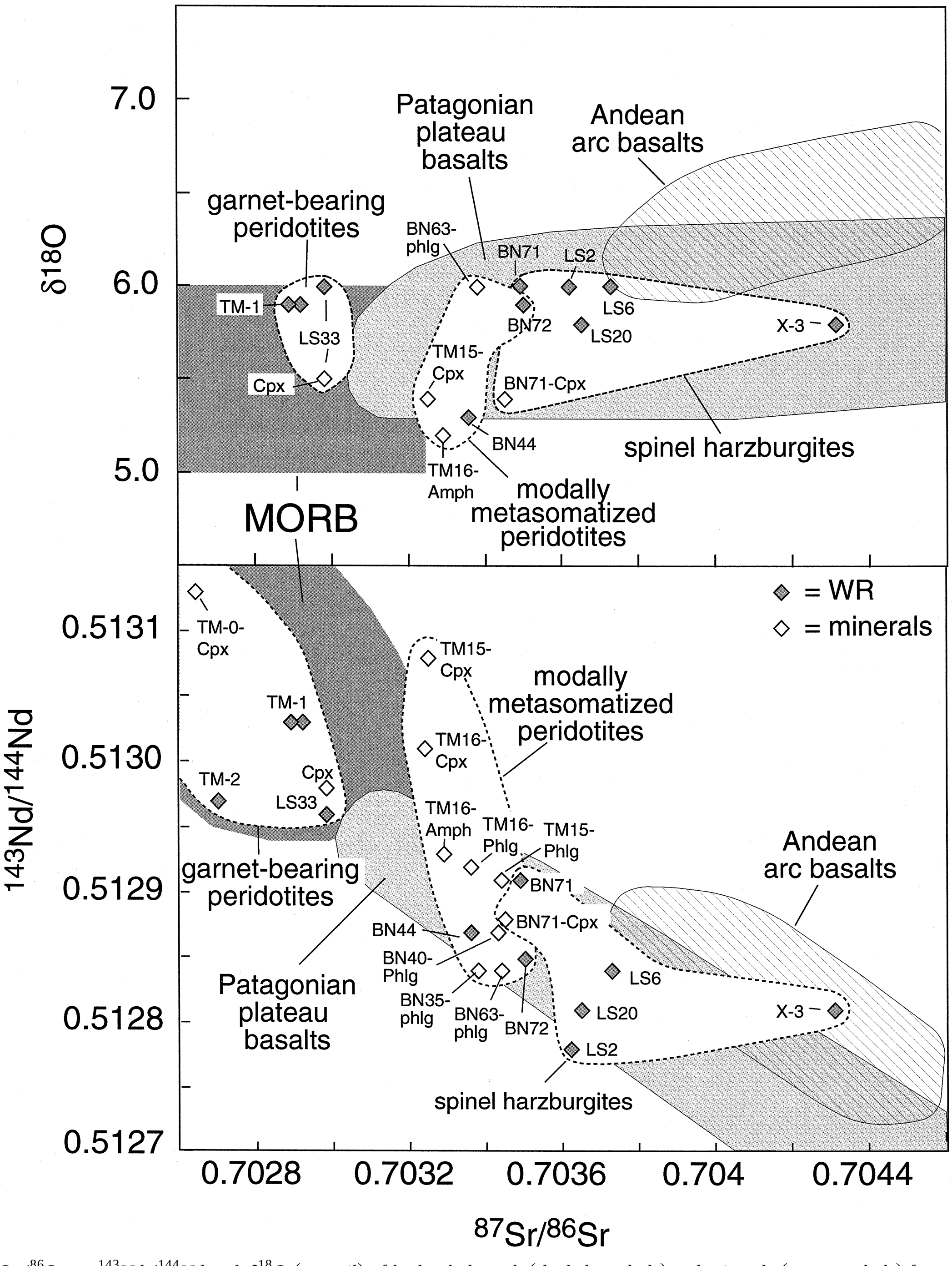

Fig. 7. $^{87}Sr/^{86}Sr$ vs. $^{143}Nd/^{144}Nd$ and $\delta^{18}O$ (per mil) of both whole-rock (shaded symbols) and minerals (open symbols) from Pali-Aike peridotite xenoliths compared to MORB (Bach et al., 1994), Patagonian plateau alkali basalts (Stern et al., 1990) and Andean arc basalts (Futa and Stern, 1988; Lopez-Escobar et al., 1993). Unveined garnet lherzolites have Sr, Nd and O isotopic compositions similar to MORB. Vein phlogopite and amphibole, and modally metasomatized lherzolites, have isotopic compositions more similar to Pali-Aike and other Patagonian plateau alkali basalts, as do cryptically metasomatized spinel harzburgites.

Table 4
U, Th and Pb concentrations, in ppb, and Pb isotopic compositions of minerals in Pali-Aike peridotite xenoliths (Gt = garnet; Sp = spinel; Cpx = clinopyroxene; Phlg = phlogopite mica)

Sample	U	Th	Pb	$^{206}Pb/^{204}Pb$	$^{207}Pb/^{204}Pb$	$^{208}Pb/^{204}Pb$
Garnet peridotites (unveined)						
LS-33 Cpx	12.67	57.56	27.24	18.07	15.40	37.61
LS-33 Gt	8.77	10.21	0.93	18.26	15.39	37.77
Spinel + garnet peridotites (unveined)						
TM-0 Cpx	46.13	190.50	83.70	18.40	15.49	38.00
Modally metasomatized (veined) peridotites						
TM-16 Cpx	13.47	46.22	61.62	18.95	15.56	38.51
TM-16 Phlg	–	103.7	423	18.77	15.57	38.50
BN-96 Phlg	–	–	360	19.23	15.62	38.80

Table 5
Os concentrations, isotopic ratios and ''rhenium depletion'' model ages for Pali-Aike xenoliths

Sample	Os (ppb)[a]	$^{187}Os/^{188}Os$[a]	Model ages (Ma)[b]
Garnet peridotite			
LS-33	2.748	0.1231	860
TM-17	2.992	0.1282	140
Spinel + garnet peridotite			
TM-0	0.774	0.1280	173
TM-1	1.543	0.1293	0
TM-2	2.568	0.1255	531
Spinel peridotite			
BN-71	3.227	0.1185	1500

[a] Determined as described in Hauri and Hart (1993).
[b] Re–Os model ages calculated assuming Re/Os = 0 as described by Walker et al. (1989).

Nd, Pb and O isotopic compositions similar to Pali-Aike and other Patagonian alkali olivine basalts (Tables 3, 4 and 6; Figs. 7 and 8). $^{87}Sr/^{86}Sr$ ratios in phlogopites are higher than both co-existing amphibole and Pali-Aike basalts, but this may reflect their

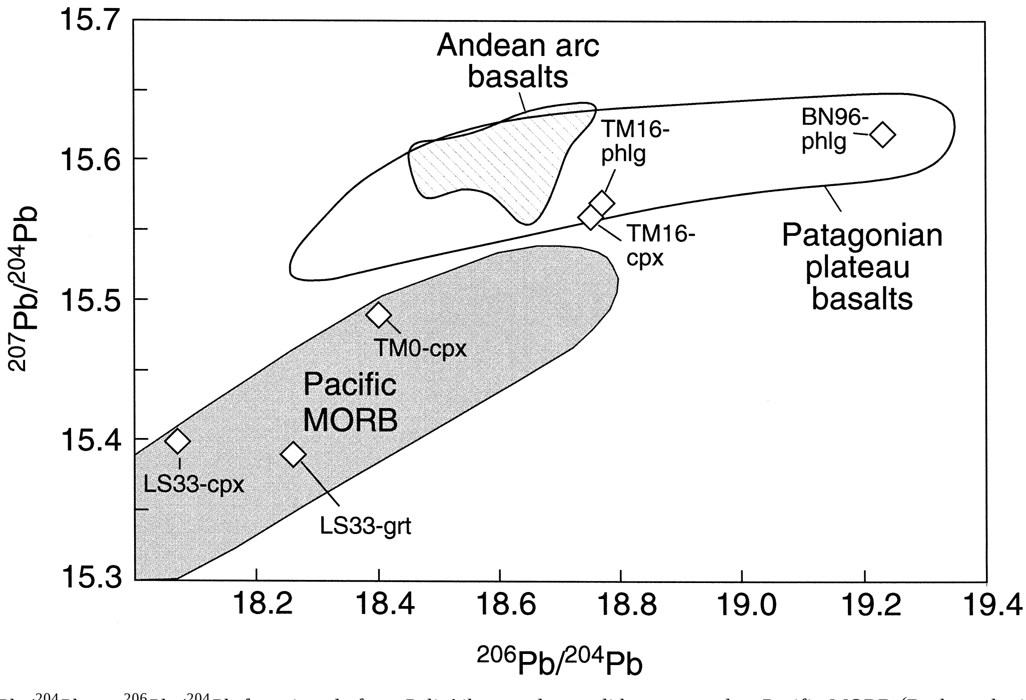

Fig. 8. $^{207}Pb/^{204}Pb$ vs. $^{206}Pb/^{204}Pb$ for minerals from Pali-Aike mantle xenoliths compared to Pacific MORB (Bach et al., 1994; Klein and Karsten, 1995), Patagonian plateau alkali basalts (Stern et al., 1990), and Andean arc basalts (Lopez-Escobar et al., 1993). Fertile garnet-bearing lherzolites (LS33 and TM0) have Pb isotopic compositions similar to MORB, while metasomatic vein phlogopite and clinopyroxene in a xenolith (TM16) with veins have Pb isotopic compositions within the field of Pali-Aike and other Patagonian plateau alkali basalts.

Table 6
$\delta^{18}O$ and δD, in parts-per-mil, for minerals in Pali-Aike xenoliths (Ol = olivine; Opx = orthopyroxene; Cpx = clinopyroxene; Gt = garnet; Sp = spinel; Phlg = phlogopite mica; Amph = pargasitic amphibole; WR = whole-rock calculated based on modal proportions of constituent minerals)

Sample	Ol	Opx	Cpx	Gt	Sp	Amph	Phlog	δD	WR*$\delta^{18}O$
Garnet peridotites (unveined)									
LS-33	6.4	5.5	5.5	6.2	–	–	–	–	6.0
Spinel + garnet peridotites (unveined)									
TM-1	5.8	6.0	6.0	5.9	–	–	–	–	5.9
Spinel peridotites (unveined)									
LS-2	6.1	6.1	5.7	–	–	–	–	–	6.0
LS-6	6.0	6.0	5.9	–	5.1	–	–	–	6.0
LS-20	5.8	5.7	5.5	–	–	–	–	–	5.8
BN-71	6.3	5.4	5.4	–	5.4	–	–	–	6.0
X-3	5.8	5.6	5.8	–	5.0	–	–	–	5.8
Modal metasomatized (veined) peridotites									
BN-35	6.1	6.2	5.2	6.0	–	–	5.4	−112	6.0
BN-55	5.6	5.5	–	5.9	–	–	5.4	−56	5.6
BN-72	6.1	5.3	5.6	–	–	–	5.5	–	5.9
BN-44	5.2	5.4	–	–	–	–	5.5	−66	5.3
BN-40	5.0	5.4	–	–	–	–	5.7	−125	5.2
BN-51	5.4	5.5	–	–	–	–	5.7	−56	5.5
BN-46	–	5.4	–	6.0	–	–	5.5	−67	5.6
BN-42	–	5.2	–	5.4	–	–	6.4	–	5.3
BN-13	–	6.3	–	5.7	–	–	5.8	–	6.0
TM-14									
Above	5.9	5.5	–	5.8	–	–	–	–	5.7
Vein	–	6.1	–	–	–	–	6.8	–	6.5
Vein	–	–	–	–	–	–	6.5	–	6.5
Below	5.5	5.5	–	5.7	–	–	–	–	5.6
TM-15									
Vein	5.7	5.3	–	5.4	–	5.2	5.4	–	5.4
Below	5.2	5.3	–	–	–	–	–	–	5.2
Away	5.6	5.3	–	–	–	–	–	–	5.5
Eclogite / pyroxenite									
BN-49	–	–	5.5	5.9	–	–	–	–	5.7
BN-25	–	5.9	–	5.8	–	–	–	–	5.9
LS-3	–	5.3	–	5.0	–	–	–	–	5.2
BN-35	6.1	6.2	5.2	6.0	–	–	5.4	−112	6.0

high Rb/Sr ratios (Stern et al., 1989). These modal metasomatic minerals are isotopically unlike Andean arc basalts, as are Pali-Aike alkali basalts (Stern et al., 1990), and provide no evidence for the introduction of any slab-derived fluids into the continental lithosphere below the Pali-Aike volcanic field, which is located > 200 km east of the Andean arc of andesitic volcanoes (Fig. 1). Also, no highly radiogenic phases preserving heterogeneities produced by ancient enrichment events occur in the Pali-Aike xenoliths.

Clinopyroxenes separated from close to veins in two modally metasomatized garnet-bearing peridotites (TM15 and TM16; Tables 3 and 4) have Sr and Pb isotopic compositions similar to vein minerals, but Nd isotopic compositions more similar to unveined garnet-bearing peridotites (Figs. 7 and 8), possibly reflecting the relatively high Sr and Pb content of vein minerals relative to peridotite. Oxygen isotopes of minerals in and around a vein in one sample (TM15; Table 6) appear to have equilibrated, while in another vein (TM14) they have not (Kyser, 1990). These data suggest variable amounts of centimeter-scale diffusion of these elements from the veins into the surrounding mantle, with diffusion rates for different elements presumably dependent on concentration gradients and temperature.

LAM–ICP–MS analysis indicate that the trace-element composition of cores of clinopyroxenes in spinel harzburgites are similar to those of clinopyroxenes in garnet lherzolites. However, incompatible trace-elements are enriched at the rims compared to the cores of the clinopyroxenes in these low- and moderate-temperature spinel harzburgites (Fig. 6). This suggests possibly meter to kilometer-scale cryptic metasomatism, since these xenolith typically contain no evidence of modal metasomatism. Although the concentration of modal metasomatic veins is greatest among high-temperature xenoliths derived from the deepest portion of the lithosphere, such zoning in high-temperature garnet lherzolites is apparently absent within detection limits (Fig. 6). This may reflect the more rapid diffusion and equilibration rates at higher temperatures deeper in the mantle.

3. Discussion and conclusions

The core-to-rim chemical zonation of orthopyroxenes (Fig. 4) suggest a complex thermal history for the Pali-Aike peridotite xenoliths, as does the textural evidence for the reaction spinel + pyroxene ⇒ garnet + olivine preserved in spinel + garnet peridotites, and the reverse reaction as indicated by spinel and pyroxenes in kelyphitic rims around some garnets (Fig. 3). Since diffusion and exchange of Mg between pyroxenes is more rapid than Ca diffusion, and the Ca diffusion is slower in orthopyroxene than clinopyroxene (Sautter and Harte, 1988; Witt-Eickschen and Seck, 1991; Werling and Altherr, 1997), we have used the differences in the T estimates based on the Ca-in-orthopyroxene thermometer compared to the two-pyroxene thermometer (Brey and Köhler, 1990) to constrain the thermal history of the Pali-Aike xenoliths (Fig. 9).

Fig. 4 shows that for the spinel harzburgite LS2, the temperatures estimated by the Ca-in-orthopyroxene thermometer decrease from the core to the rim by 135°C. In contrast, temperatures estimated by the two-pyroxene thermometer are uniform throughout the crystal, and 175°C (±32°C) lower in the core compared to those estimated by the Ca-in-orthopyroxene thermometer. We interpret these differences as due to incomplete equilibration of Ca in orthopyroxene compared to Mg exchange between the two pyroxenes during cooling of the xenolith LS2 by at least 175°C (Fig. 9a). Other indications of significant cooling of the lithosphere below Pali-Aike include both the textural evidence for the reaction spinel + pyroxene ⇒ garnet + olivine preserved in the spinel + garnet peridotites (Fig. 3), and the exsolution of clinopyroxene from orthopyroxene, and vice versa, observed in many low-temperature (< 970°C based

Fig. 9. P–T history of the lithosphere below southern South America, based on mineral thermometry (Fig. 4), mineralogic evidence for reactions due to either heating or cooling, and geologic constraints which indicate 7 km of sedimentation in the Magellanes basin since the Jurassic breakup of Gondwanaland (Biddle et al., 1986), when widespread magmatic mafic and silicic magmatic activity associated with extension heated and thinned the lithosphere (Bruhn et al., 1978). Subsequent to this heating event, an early period of long term cooling, of up to 175°C (arrow a; Fig. 9a), is documented in low-T spinel peridotites (LS2, Fig. 4) and websterites (open square) by differences between core temperatures, estimated with the Ca-in-orthopyroxene thermometer, compared to rim temperatures, estimated with the two-pyroxene thermometer (Fig. 4 and inset). This cooling also produced the reaction spinel + pyroxene ⇒ garnet + olivine, as spinel lherzolites cooled across the dotted reaction line separating spinel from garnet peridotites (Webb and Wood, 1986). Prior to cooling, the subcontinental geotherm was similar to the 75 mW m^{-1} geotherm of Chapman (1986), and the lithosphere was approximately 80 km thick. After cooling the geotherm was closer to the 65 mW m^{-1} geotherm (Fig. 2). Recent heating of up to > 65°C (arrow b; Fig. 9b) is documented in high-temperature garnet-bearing peridotites (open triangles and circles) by differences between core temperatures, estimated with the Ca-in-orthopyroxene thermometer, compared to rim temperatures, estimated with the two-pyroxene thermometer (Fig. 4 and inset). This heating, which may be related to the generation of the Pali-Aike basalts, also produced spinel + pyroxene in kelyphitic rims surrounding garnets, and has thinned the lithosphere to < 100 km.

on the two-pyroxene thermometer) pyroxenites, websterites and spinel peridotites. Selverstone and Stern (1983) also documented cooling in deep-crustal metabasic granulite xenoliths, based on both mineral

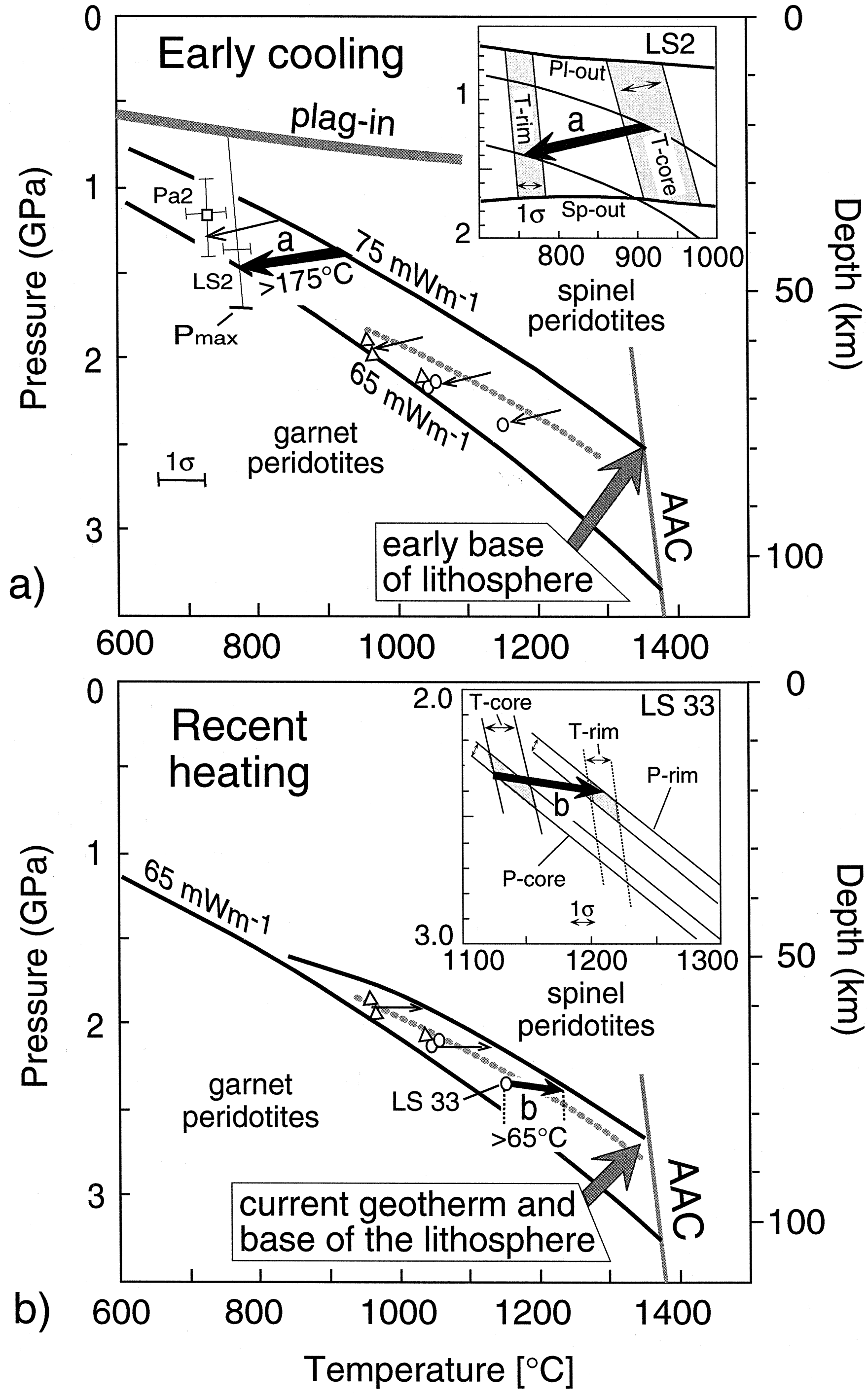

thermometry and fluid inclusions in granoblastic pyroxenes compared to pyroxenes in symplectic intergrowths formed by reaction of plagioclase and olivine.

The timing of this cooling event is uncertain, but for similar chemical zonation patterns in orthopyroxenes within low-*T* (≈ 800°C) peridotite xenoliths from the East African Rift system, Garasic (1997) calculated cooling times of 200 to 500 Ma based on cation diffusion models for Ca and Al in orthopyroxene. This suggests that the chemical zonations observed in orthopyroxenes within low-*T* Pali-Aike xenoliths reflect slow, long-term cooling. Geologic constraints suggest that long-term cooling has occurred below southernmost South America since the Jurassic, when widespread mafic and silicic volcanism was associated with the extensional break-up of Gondwanaland (Bruhn et al., 1978). Since this event the area in which the Pali-Aike basalts erupted has been a slowly subsiding sedimentary basin without any magmatic activity until the Quaternary (Biddle et al., 1986).

In contrast to the low-*T* xenoliths, chemical zoning in orthopyroxene within high-*T* garnet peridotites (Fig. 4) suggests a heating event. In garnet lherzolites, temperatures estimated by the Ca-in-orthopyroxene thermometer increase from core-to-rims, and temperatures estimated by the two-pyroxene thermometer are uniformly higher. The difference between core temperatures estimated by the Ca-in-orthopyroxene thermometer, compared to rim temperatures estimated by the two-pyroxene thermometer, is 65°C (±32°C) for garnet lherzolite LS33, the highest temperature xenolith documented from Pali-Aike (Figs. 2 and 4). Some garnet-bearing lherzolites show core-to-rim temperature increases up to 90°C (Fig. 9b). However, the flat/or parabolic shape of the Ca zonation pattern in orthopyroxenes within high-*T* garnet lherzolites (Fig. 4), suggests that the lowest temperatures reached by these xenoliths prior to heating is not preserved in the core composition, and the amount of heating calculated is a minimum. Other evidence for heating of high-*T* garnet-bearing peridotites are kelyphitic rims, containing spinel and pyroxenes, developed around garnets. This indicates the occurrence of the reaction garnet + olivine ⇒ spinel + pyroxene, which implies either heating (Fig. 9b) or decompression. These kelyphitic rims occasionally contain unzoned grains of pargasitic amphibole similar in composition to amphibole both in veins and occurring as isolated grains, which suggests that these rims did not form solely during decompression associated with the transport of the xenoliths to the surface.

Based on the significantly higher diffusion rates of Ca and Al at high temperatures, this heating event is considered to be a more recent event, possibly related to the generation of the Pali-Aike basalts, than the cooling which produced the inverse chemical zonation patterns in orthopyroxenes within low-*T* Pali-Aike xenoliths. The low-*T* xenoliths apparently have not yet been affected by this heating. The different zonation patterns of Ca and Al in orthopyroxenes of both low- and high-temperature xenoliths which occur together in the same host basalts, as well as the shape of the zonation patterns in the high-*T* xenoliths, argue against the possibility that the recent heating of the high-*T* peridotites was caused during xenolith transport to the surface in the host magma.

We conclude that after the Jurassic, when it was thinned by extensive magmatic activity and extension, the lithosphere below southernmost South America cooled by as much as 175°C and thickened from approximately 80 to 100 km (Fig. 9a). More recently, it has been heated by a minimum of 65°C and thinned again to < 100 km (Fig. 9b). Since element diffusion and equilibration is strongly temperature dependent (Crank, 1975; Jurewicz and Watson, 1988), evidence for the earlier cooling event is preferentially preserved in low-temperature xenoliths from shallower in the mantle, while evidence for the more recent heating event is reflected in high-temperature xenoliths from deeper in the mantle.

From a global perspective, these changes in geothermal gradient and thickness are relatively minor, and no evidence preserved in the Pali-Aike xenoliths suggests that the subcontinental lithosphere beneath southernmost South America was ever significantly thicker than oceanic lithosphere beneath > 100 Ma oceanic crust. Its current geothermal gradient and lithospheric thickness is more similar to oceanic lithosphere than Archean continental lithosphere.

Furthermore, the types of lithologies found among the Pali-Aike peridotite xenoliths, and their vertical distribution in the lithosphere as deduced from the

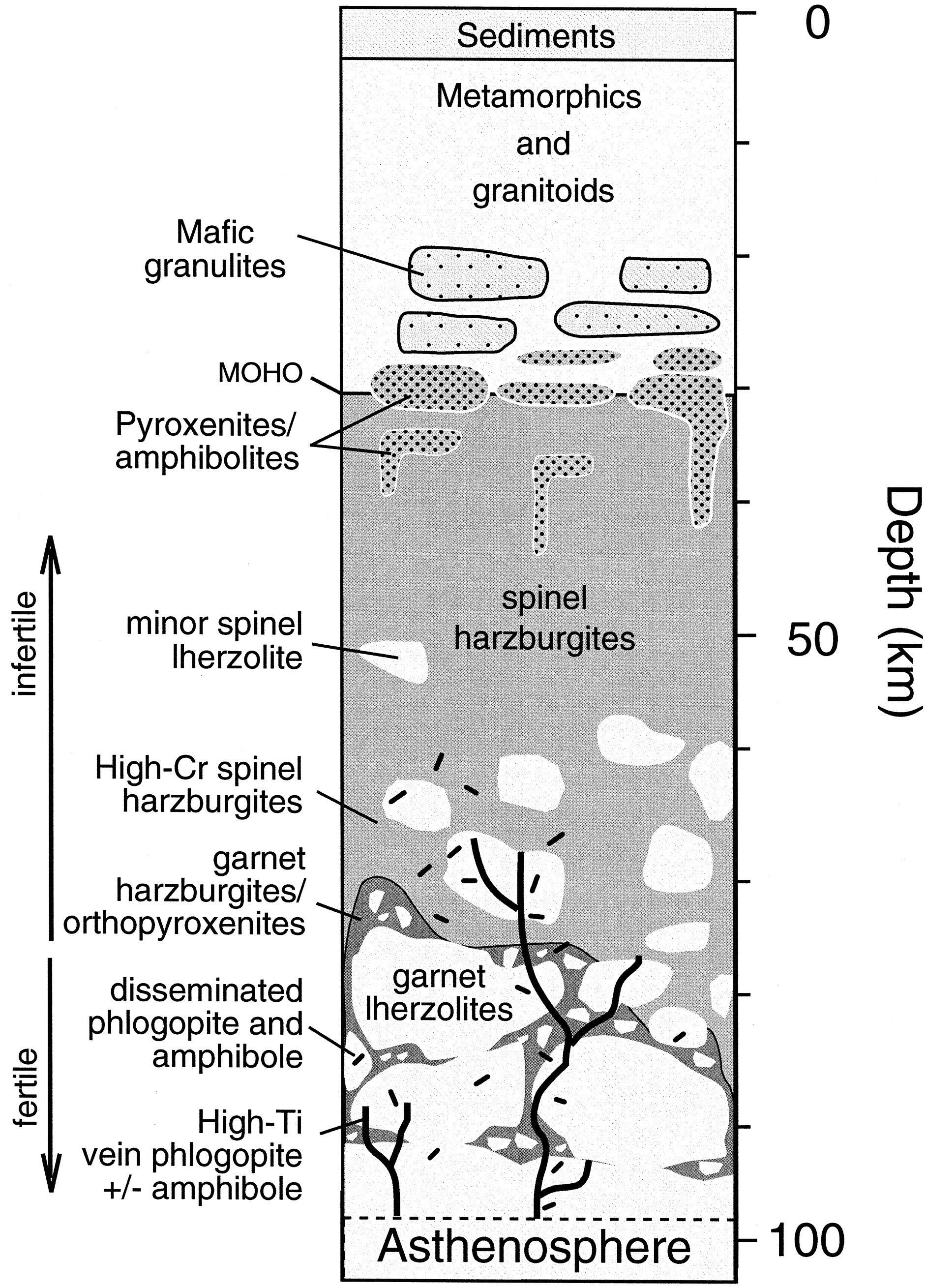

Fig. 10. Lithologic zonations, modified after Stern et al. (1986, 1989), of the continental lithosphere of southernmost South America as suggested by the calculated temperature and pressure of equilibration of Pali-Aike xenoliths. Mafic granulites occur in the deeper portion of the continental crust (Selverstone and Stern, 1983). Infertile spinel harzburgites are predominant in the upper and middle section of mantle, whereas the deepest portion of the lithosphere consists dominantly of fertile garnet lherzolites. The lower lithosphere was modified by both modal and cryptic metasomatism related to the generation of the Pali-Aike basalts.

estimates of their temperature and pressure (Fig. 10), are similar to that expected for oceanic lithosphere, and different from that described for Archean continental lithosphere (Stern et al., 1986, 1989; Henjes-Kunst and Altherr, 1992). Low-temperature (< 970°C) xenoliths from the shallow portion of the mantle lithosphere are predominantly infertile spinel harzburgites. Although some harzburgites also occur among moderate- and high-temperature (> 970°C) xenoliths, these high-temperature xenoliths from the deeper portion of the lithosphere are predominantly fertile spinel + garnet and garnet lherzolites with trace-element and isotopic compositions similar to the mantle source of mid-oceanic ridge basalts. This implies a significant continuous chemical and density gradient, over a relatively short vertical distance of a few tens of kilometers, with decreasing olivine and increasing clinopyroxene and garnet content, and thus increasing density with depth.

The apparent continuous nature of the vertical transition in the upper 50 km of the mantle below southernmost South America, from infertile harzburgite to more fertile lherzolite (Fig. 10), has been explained by magma extraction from the shallow portion of the lithosphere at a late Proterozoic mid-oceanic spreading center, prior to the tectonic capture and accretion of this mantle section to the western margin of Gondwanaland during the Paleozoic (Stern et al., 1986, 1989). Re/Os model ages (Table 5) are consistent with this explanation. An alternative model, in which the lower fertile portion of this lithosphere has been underplated below older, refractory lithosphere, may be possible, but nevertheless, no evidence exists that the shallow refractory portion of this lithosphere was ever greater in thickness than 80 km.

In summary, there is no evidence from the Pali-Aike xenoliths for the existence of a thick, olivine-rich, lithospheric mantle root below southernmost South America, either currently or in the past. The highest temperature garnet lherzolites derived from the deepest sampled portion of this lithosphere are mineralogically and chemically similar to the global asthenospheric source of MORB, and the transition from lithosphere to asthenosphere, which currently occurs at < 100 km, must reflect temperature and rheology rather than chemistry and/or density. The mineralogic evidence for a multi-stage thermal history of this lithospheric section suggests that this temperature/rheology dependent transition between the lithosphere and asthenosphere below southernmost South America has migrated both upwards and downwards by a few tens of kilometers with time, and that the current lithosphere cannot be considered a permanent root.

Acknowledgements

The xenoliths from the Pali-Aike volcanic field were first discovered and collected in collaboration with Alexandra Skewes. Early stages of analytical work on these xenoliths was supported by NSF grants EAR79-11204 and EAR83-13884, and recent work by German Research Foundation grant AL-166/10.

References

Allègre, C.J., Poirier, J.P., Humler, E., Hofmann, A.W., 1995. The chemical composition of the earth. Earth Planet. Sci. Lett. 134, 515–526.

Bach, W., Hegner, E., Erzinger, J., Satir, M., 1994. Chemical and isotopic variations along the superfast spreading East Pacific Rise from 6 to 30°S. Contrib. Mineral. Petrol. 116, 365–380.

Biddle, K.T., Uliana, M.A., Mitchum, R.M. Jr., Fitzgerald, M.G., Wrigth, R.C., 1986. The stratigraphic and structural evolution of the central and eastern Magallanes Basin, southern South America. Int. Assoc. Sedimentol., Spec. Publ. 8, 41–61.

Brey, G.P., Köhler, T., 1990. Geothermobarometry in four-phase lherzolites: II. New thermobarometers, and practical assessment of existing thermobarometers. J. Petrol. 31, 1353–1378.

Bruhn, R.L., Stern, C.R., de Wit, M.J., 1978. Field and geochemical data bearing on the development of a Mesozoic volcano-tectonic rift zone and back-arc basin in southernmost South America. Earth Planet. Sci. Lett. 41, 32–46.

Cande, S.C., Leslie, R.B., 1986. Late Cenozoic tectonics of the southern Chile Trench. J. Geophys. Res. 91, 495–520.

Chapman, D.S., 1986. Thermal gradients in the continental crust. In: Dawson, J.B., Carswell, D.A., Hall, J., Wedepohl, K.H. (Eds.), The Nature of the Lower Continental Crust. Geol. Soc. London, Spec. Publ. 24, pp. 63–70.

Crank, J., 1975. The Mathematics of Diffusion. Oxford Univ. Press, London.

de Wit, M.J., 1977. The evolution of the Scotia arc as a key to the reconstruction of Gondwanaland. Tectonophysics 37, 53–81.

Douglas, B.J., Saul, S.L., Stern, C.R., 1987. Rheology of the upper mantle beneath southernmost South America inferred from peridotite xenoliths. J. Petrol. 95, 241–253.

Futa, K., Stern, C.R., 1988. Sr and Nd isotopic and trace element compositions of Quaternary volcanic centers of the southern Andes. Earth Planet. Sci. Lett. 88, 253–262.

Garasic, V., 1997. Mantelxenolithe als Dokumente der thermischen Entwicklung des Erdmantels unter den Chyulu Hills, Kenia. PhD Thesis. Univ. Heidelberg, 220 pp.

Hauri, E.H., Hart, S.R., 1993. Re–Os isotope systematics of HIMU and EMII oceanic island basalts from the south Pacific Ocean. Earth Planet. Sci. Lett. 114, 353–371.

Henjes-Kunst, F., Altherr, R., 1992. Metamorphic petrology of xenoliths from Kenya and northern Tanzania and implications for geotherms and lithospheric structures. J. Petrol. 33, 1125–1156.

Hofmann, A.W., 1988. Chemical differentiation of the Earth: relationship between mantle, continental crust and oceanic crust. Earth Planet. Sci. Lett. 91, 271–285.

Jackson, S.E., Longerich, H.P., Dunning, G.R., Fryer, B.J., 1992. The application of laser ablation microprobe–inductively coupled plasma–mass spectrometry (LAM–ICP–MS) to in situ trace element determinations in minerals. Can. Mineral. 30, 1049–1064.

Jurewicz, A.J.G., Watson, E.B., 1988. Cations in olivine: Part 2. Diffusion in olivine xenocrysts, with applications to petrology and mineral physics. Contrib. Mineral. Petrol. 99, 186–201.

Klein, E.M., Karsten, J.L., 1995. Ocean-ridge basalts with convergent-margin geochemical affinities from the Chile Ridge. Nature 374, 52–57.

Kyser, T.K., 1990. Stable isotopes in the continental lithospheric mantle. In: Menzies, M. (Ed.), Continental Mantle. Oxford Univ. Press, pp. 127–156.

Lopez-Escobar, L., Kilian, R., Kempton, P.D., Tagiri, M., 1993. Petrology and geochemistry of Quaternary rocks from the Southern Volcanic Zone of the Andes between 41°30′ and 46°00′S, Chile. Rev. Geol. Chile 20, 33–56.

Maaløe, S., Aoki, K.I., 1975. The major element composition of the mantle estimated from the composition of lherzolites. Contrib. Mineral. Petrol. 63, 161–173.

McDonough, W.F., 1990. Constraints on the composition of the continental lithospheric mantle. Earth Planet. Sci. Lett. 101, 1–18.

McKenzie, D., Bickle, M.J., 1988. The volume and composition of melt generated by extension of the lithosphere. J. Petrol. 29, 625–679.

Nickel, K.G., Green, D.H., 1985. Empirical geothermobarometry for garnet peridotites and implications for the nature of the lithosphere, kimberlites and diamonds. Earth Planet. Sci. Lett. 73, 158–170.

Olker, B., 1997. Druck-Temperatur-Abschätzungen an Mantelxenolithen von Pali-Aike, südliches Südamerika. Unpublished Diploma Thesis. Univ. Heidelberg, 97 pp.

Palme, H., Nickel, K.G., 1985. Ca/Al ratio and composition of the Earth's upper mantle. Geochim. Cosmochim. Acta 49, 2123–2132.

Ramos, V.A., 1988. Late Proterozoic–Early Paleozoic of South America — a collisional history. Episodes 11, 168–174.

Ringwood, A.E., 1979. Origin of the Earth and Moon. Springer-Verlag, New York.

Sautter, V., Harte, B., 1988. Diffusion gradients in an eclogite xenolith from the Roberts Victor Kimberlite Pipe: 1. Mechanism and evolution of garnet exsolution in Al_2O_3-rich clinopyroxene. J. Petrol. 29, 1325–1352.

Selverstone, J., Stern, C.R., 1983. Petrochemistry and recrystallization history of granulite xenoliths from the Pali-Aike volcanic field, Chile. Am. Mineral. 68, 1102–1112.

Skewes, M.A., Stern, C.R., 1979. Petrology and geochemistry of alkali basalts and ultramafic inclusions from the Pali-Aike volcanic field in southern Chile and the origin of the Patagonian plateau lavas. J. Volcanol. Geotherm. Res. 6, 3–25.

Stern, C.R., Kilian, R., 1996. Role of the subducted slab, mantle wedge and continental crust in the generation of adakites from the Andean Austral Volcanic Zone. Contrib. Mineral. Petrol. 123, 263–281.

Stern, C.R., Futa, K., Saul, S., Skewes, M.A., 1986. Nature and evolution of the subcontinental mantle lithosphere below southern South America and implications for Andean magma genesis. Rev. Geol. Chile 27, 41–53.

Stern, C.R., Saul, S., Skewes, M.A., Futa, K., 1989. Garnet peridotite xenoliths from Pali-Aike basalts of southernmost South America. Kimberlites and related rocks. Geol. Soc. Aust., Spec. Publ. 14. Blackwell, Carlton, Australia, pp. 735–744.

Stern, C.R., Frey, F.A., Futa, K., Zartman, R.E., Peng, Z., Kyser, T.K., 1990. Trace-element and Sr, Nd, Pb, and O isotopic compositions of Pliocene and Quaternary alkali basalts of the Patagonian Plateau lavas of southernmost South America. Contrib. Mineral. Petrol. 104, 294–308.

Taylor, S.R., McLennan, S.M., 1985. The Continental Crust: Its Composition and Evolution. Blackwell, Oxford.

Taylor, R.P., Jackson, S.E., Longerich, H.P., Webster, J.D., 1996. In situ trace element analysis of individual silicate melt inclusions by laser ablation microprobe–inductively coupled plasma–mass spectrometry (LAM–ICP–MS). Geochim. Cosmochim. Acta 61, 2559–2567.

Walker, R.J., Carlson, R.W., Shirey, S.B., Boyd, F.R., 1989. Os, Sr, Nd and Pb isotope systematics of southern African peridotite xenoliths: implications for the chemical evolution of the subcontinental mantle. Geochim. Cosmochim. Acta 53, 1583–1595.

Webb, S.A.C., Wood, B.J., 1986. Spinel–pyroxene–garnet relationships and their dependence on Cr/Al ratio. Contrib. Mineral. Petrol. 92, 471–480.

Wells, P.R.A., 1977. Pyroxene thermometry in simple and complex systems. Contrib. Mineral. Petrol. 62, 19–139.

Werling, F., Altherr, R., 1997. Thermal evolution of the lithosphere beneath the French Massif Central as deduced from geothermobarometry on mantle xenoliths. Tectonophysics 275, 119–141.

Witt-Eickschen, G., Seck, H.A., 1991. Solubility of CaO and Al_2O_3 in orthopyroxene from spinel peridotite: an improved version of an empirical geothermometer. Contrib. Mineral. Petrol. 106, 431–439.